



# Numerical predictions of flashback limits of H<sub>2</sub>-enriched methane/air premixed laminar flames

A. Cuoci<sup>a,\*</sup>, A. Frassoldati<sup>a</sup>, F. Cozzi<sup>b</sup>

<sup>a</sup> CRECK Modeling Lab, Department of Chemistry, Materials, and Chemical Engineering, Politecnico di Milano, Italy

<sup>b</sup> Department of Energy, Politecnico di Milano, Italy

## ARTICLE INFO

### Keywords:

Hydrogen  
Flashback  
Burner  
Natural gas  
Decarbonization

## ABSTRACT

Hydrogen is considered as a promising resource for decarbonizing not just the industrial sector but also domestic heating systems. By partially substituting natural gas with hydrogen, domestic combustion-based conversion systems have the potential to enhance efficiency, decrease carbon emissions, and achieve cleaner combustion, specifically reducing levels of particulate matter. Nevertheless, hydrogen possesses properties that differ significantly from natural gas. In particular, due to its higher laminar flame speed, hydrogen has a much higher propensity to *flashback* than natural gas, raising notable safety concerns.

This study aims to examine the impact of H<sub>2</sub> addition (up to 100%) to natural gas on the combustion process in domestic condensing boilers. To achieve this objective, 3D numerical simulations are conducted, modeling the multi-hole geometry that emulate perforated burners commonly found in these appliances. The simulations incorporate detailed kinetics and conjugate heat transfer with the burner plate and consider various hole-to-hole distances for a more comprehensive analysis. Flashback limits are found for a wide range of operating conditions of interest for domestic applications, with equivalence ratios from 0.5 to 1 and hydrogen fractions from 0 (pure methane) to 1 (pure hydrogen).

The results confirm the observations of previous works on planar, multi-slit configurations. More specifically, the results show that the conventional flashback correlation based on the concept of *critical velocity gradient* becomes inaccurate for H<sub>2</sub> fractions larger than 0.50 as it does not take into account stretch induced preferential diffusion effects, which are especially large in the multi-hole configuration here investigated.

## 1. Introduction

Fossil fuels, which have powered the world since the industrial revolution, are a major source of greenhouse gases (GHG) that contribute to global warming. To address this issue, alternative energy sources must be developed to replace fossil fuels, especially in sectors such as residential heating, where significant energy consumption is attributed to gas boilers.

The current status of residential heating reveals a substantial reliance on natural gas (NG) and fossil fuels more in general. According to the Annual Energy Outlook [1], as of 2022, approximately 49% of U.S. households rely on NG for heating. Similarly, in Europe, NG stands as the main source for residential heating [2]. However, the wide adoption of NG comes with significant environmental consequences. The combustion of NG accounted for 7.5 Gtons of CO<sub>2</sub> emissions on a global scale in 2021 [1]. Moreover, the heating sector faces persistent challenges pertaining to energy efficiency. Traditional heating systems, including older models that continue to operate, exhibit large

inefficiencies. These systems operate with efficiency levels that can drop to 56% [3]. In contrast, modern condensing boilers, frequently incorporating perforated burners, could achieve efficiencies up to 98%. This improvement in energy efficiency proves instrumental in reducing energy waste and the associated carbon emissions.

One approach to promote decarbonization and reduce the carbon footprint of heating systems is the adoption of zero carbon-ready gas boilers that utilize green hydrogen as a fuel, generated through renewable energy sources such as wind and solar power. Blending H<sub>2</sub> into the existing gas network is expected to provide an efficient means of dealing with the variability and intermittency of renewable energy sources [4].

However, H<sub>2</sub> presents unique challenges due to its peculiar properties compared to NG. The differences in properties, such as its low molecular weight (and its associated Lewis number), contribute to variations in combustion characteristics. The impact of H<sub>2</sub> on the maximum temperature, pollutant emissions, and heat exchange in domestic

\* Corresponding author.

E-mail address: [alberto.cuoci@polimi.it](mailto:alberto.cuoci@polimi.it) (A. Cuoci).

appliances presents further concerns. Indeed,  $H_2$  high reactivity and adiabatic flame temperature make its combustion behavior distinct from that of other fuels.  $H_2$  flame speed is approximately six times higher than that of NG at stoichiometric conditions, making flame propagation and stability a complex concern, especially in premixed configurations [5]. Modern domestic heating devices, like condensing boilers, rely on premixed configurations with burners that generate short-length flames suitable for compact combustion chambers. These burners were originally designed with conventional fuels, such as NG, and their safety and performance in the context of  $H_2$  blending remains uncertain.

An undesirable phenomenon, known as *flashback*, may occur when the flame propagates upstream into burner components, creating a significant safety risk. Evaluating flashback in practical applications presents challenges due to the complex nature of the phenomenon. The laminar flame speed  $s_L$ , a crucial parameter in predicting flashback, may not fully capture the dynamics of flashback in real devices. Factors like fuel properties, flame-wall interactions, flame curvature, preferential diffusion, and stretch rate also significantly influence flashback onset [6].

Flame stabilization and flashback/blow-off limits in premixed flames were systematically studied by Lewis and Von Elbe, who proposed the first flame stabilization theory [7]. However, their theory for boundary flashback is only applicable to flame holders with negligible thickness. Despite extensions and improvements proposed during the years (see for example [8]), a comprehensive understanding of flashback phenomena for real-world applications is still lacking.

Recently, Vance et al. [5], Flores-Montoya et al. [6] and Fruzza et al. [9] studied the flashback limits of premixed  $H_2$  and  $H_2/CH_4$  flames in multi-slit burners, modeling both fluid and solid regions, including conjugate heat transfer (CHT) in their investigation. Their results confirmed that the laminar flame speed can only provide a limited indication of the flashback velocity, and highlighted the key-role played by the strong interactions between the flame and the wall. More specifically, it was demonstrated that flashback propensity of  $H_2$  flames is promoted by preferential diffusion effects and not exclusively linked to their increased flame speed.

In this study, our objective is to estimate the flashback limits for a multi-hole perforated burner fed with  $H_2$ -enriched methane/air mixtures at various equivalence ratios. To achieve this, we employ transient laminar Computational Fluid Dynamics (CFD) simulations incorporating detailed kinetics and conjugate heat transfer (CHT). The primary novelty, in comparison to previous numerical studies on the same topic [5,6,9], lies at the geometrical level. Instead of considering a planar, multi-slit configuration, our work investigates a three-dimensional configuration with circular holes. Notably, this multi-hole configuration, commonly utilized in perforated burners, has never been systematically studied to identify the flashback limits of  $H_2$ -enriched fuel mixtures, adding a unique dimension to the existing body of research.

## 2. Physical and numerical model

In this work, we numerically investigated the flashback limits occurring on a multi-hole configuration, representing a portion of a real burner adopted for domestic boilers.

### 2.1. Computational domain and mesh

A 3D computational domain, including the burner plate, was considered, as shown in Fig. 1. In order to minimize the influence of boundary conditions, the domain extends 15 mm downstream and 5 mm upstream. Thanks to the regular pattern of holes, the computational domain includes only one quarter of a single circular hole. This choice is convenient from the computational point of view because it reduces the computational time, but it does not allow to capture

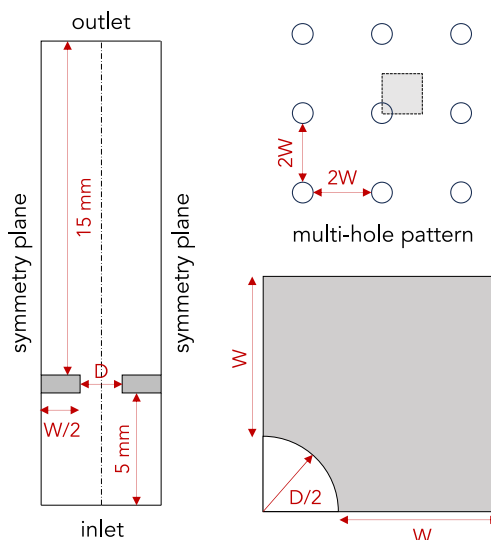


Fig. 1. Vertical and horizontal sections of the computational domain (not in scale) and multi-hole pattern adopted in the present study.

Table 1

Investigated geometrical patterns.  $A_s/A_h$  is the ratio between the cross section area corresponding to the solid plate  $A_s$  and the cross section area of holes  $A_h$ .

Pattern	$D$ (mm)	$W$ (mm)	$A_s/A_h$
A	0.8	1.5	27.72
B	0.8	1.0	14.59
C	0.8	0.5	5.44

asymmetric flashback phenomena, which have been reported by several authors [9,10]. Since the focus of the present work is not about the dynamics of flashback, the reduced computational domain here adopted can be considered a reasonable choice. Premixed gases enter from the bottom with a uniform inlet velocity normal to the inlet section and temperature  $T_u$  of 300 K. Symmetry conditions are applied along the 4 vertical planes of the domain, in order to mimic the multi-hole nature of the perforated burner. Conjugate Heat Transfer (CHT) between the fluid region and the plate burner (solid region) is included. As widely demonstrated in the literature [5,6,9], heat exchange with the burner plate plays a key-role on the flashback limits. The burner plate, whose thickness is fixed and assumed equal to 0.6 mm, is modeled using the properties of stainless steel usually adopted in domestic boilers:  $\rho = 7700 \text{ kg/m}^3$ ,  $C_p = 460 \text{ J/kg/K}$ , and  $\kappa = 25 \text{ W/m/K}$ . At the outlet section, Neumann's boundary conditions are applied for all the variables, with the exception of pressure, which is fixed to 1 atm. No-slip boundary conditions are applied on the inert solid surface. The geometrical parameters of the burner are reported in Fig. 1 and Table 1. More specifically, the hole diameter  $D$  was kept constant and equal to 0.8 mm. This is a typical size adopted in perforated burners for domestic boilers. Three different distances  $2W$  between the holes were considered, to investigate the impact of geometrical changes on the flashback limits. Geometrical pattern A, with  $W = 1.5 \text{ mm}$ , was assumed as the reference case.

The computational mesh includes hexahedral cells only. A non-uniform cell size is adopted, in order to ensure high accuracy in the regions close to the burner plate and along the flame front. Preliminary 1D simulations of freely propagating laminar premixed flames fed with pure  $H_2$  were carried out to identify the thermal flame thickness and a proper cell size [9]. More specifically, the cell size was chosen to have at least 10 cells within the thermal flame thickness  $\delta_T$ , which was calculated as  $\delta_T = \frac{T_b - T_u}{|dT/dx|_{max}}$ , where  $T_b$  and  $T_u$  are the temperatures of burnt and unburnt gases, respectively, and  $|dT/dx|_{max}$  the maximum temperature gradient. The largest mesh (corresponding to geometry A)

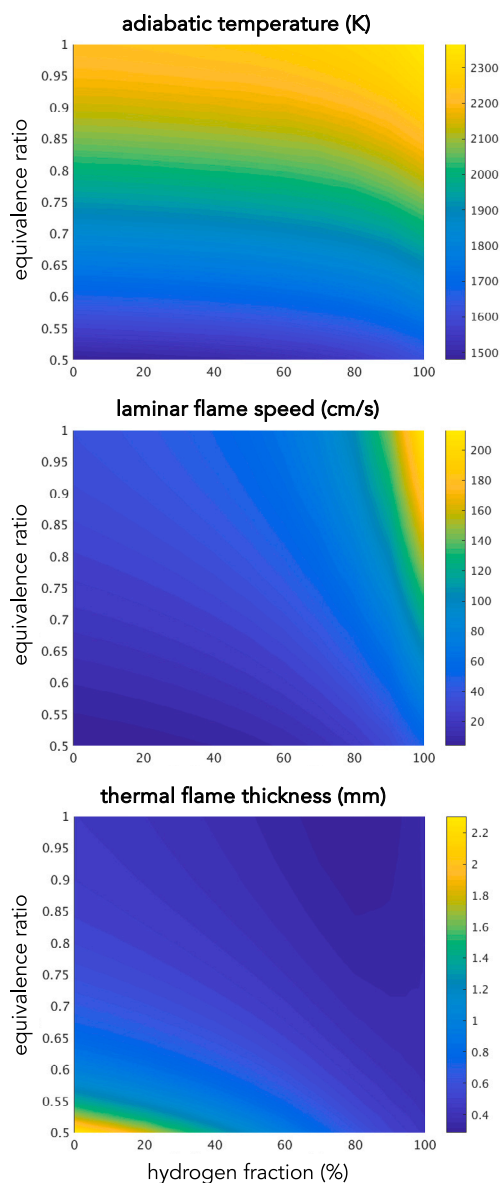


Fig. 2. Properties of  $\text{CH}_4/\text{H}_2$  mixtures as a function of equivalence ratio  $\phi$  and  $\text{H}_2$  molar content at atmospheric pressure for conditions of relevance for domestic burners: adiabatic flame temperature  $T_{ad}$ , laminar flame speed  $s_L$  and thermal flame thickness  $\delta_T$ .

contains  $\sim 40\text{k}$  cells. Sensitivity to the grid was performed on the most challenging scenario (pure  $\text{H}_2$  at  $\phi = 1.0$ ).

## 2.2. Physical model

The flow regime is laminar: the Reynolds' number calculated at the basis of burner holes ranges from  $\sim 150$  to  $\sim 1200$  (according to the specific operating conditions). No instabilities were observed, as confirmed in previous similar modeling works on multi-slit burners [5,6,9]. The conventional transport equations for momentum, species, and energy were solved using laminarSMOKE++, a CFD code based on OpenFOAM, specifically conceived for modeling laminar flows with detailed kinetic mechanisms in arbitrarily complex, multidimensional geometries [11, 12]. The diffusion fluxes were modeled using the mixture-average formulation [13] including a corrective velocity [14] to ensure conservation of mass. The Soret effect, which is expected to play a relevant role when  $\text{H}_2$  is used as a fuel, was also included. No radiative heat

transfer was included in the simulations. This is not a significant limitation in the context of domestic applications, for which non-sooting flames are expected. In addition, since radiation from the solid is an overall loss, neglecting radiation (like in the present work) implies that the burner temperature is overestimated, which therefore represent a worst-case scenario for flashback occurrence. Gravitational and viscous work effects were not modeled, as they were found not to play a significant role [5]. A reduced version of the CRECK mechanism for  $\text{CH}_4/\text{H}_2$  mixtures was considered. The reduced mechanism was obtained by applying reduction via DRG and sensitivity analyses using the DoctorSMOKE++ platform [15], targeting at conditions relevant for premixed combustion of lean  $\text{CH}_4/\text{H}_2$  mixtures at atmospheric pressure. The reduced mechanism includes 25 species and 177 reactions.

## 2.3. Coupling strategy

In this work the objective is to calculate the steady-state solutions until flashback occurs. Since the characteristic times of evolution of gaseous and solid regions are very different, the time solution of transport equations in the gaseous phase can be de-synchronized from the solid region. This means that at each time step (which is of the order of  $10^{-6}/10^{-7}$  s), the energy equation in the solid regions is solved directly in its steady-state formulation. A similar methodology has been successfully used in similar works [6,9].

## 2.4. Identification of flashback limits

The simulations were carried out in a wide range of operating conditions. More specifically, mixtures with increasing molar fraction  $\alpha$  of  $\text{H}_2$  were considered, from 0 to 1. For each mixture, equivalence ratios  $\phi$  from 0.50 to 1 were studied. In addition, pure  $\text{H}_2$  flames ( $\alpha = 1$ ) in the two additional geometries described in Table 1 were studied.

For every combination of  $\alpha$  and  $\phi$ , a sufficiently high inlet velocity was assumed and a steady state flame at thermal equilibrium with the solid plate was calculated. Then, the inlet velocity was reduced in steps corresponding to a decrease of the specific thermal power by  $\Delta P = 0.25 \text{ W/mm}^2$ . The flame and the burner temperature are allowed to stabilize by reducing the specific power (i.e., the inlet velocity), until the occurrence of flashback. The minimal, specific power at which a steady-state solution can be still obtained before flashback is designated as the flashback limit and referred to as  $P_{FB}$ .

## 3. Results and discussion

### 3.1. Preliminary analyses

Preliminary analyses were carried out in order to assess the most relevant combustion properties of  $\text{CH}_4/\text{H}_2$  mixtures (with  $\alpha$  from 0 to 1) in lean conditions of relevance for applications in domestic burners. Fig. 2 reports the adiabatic temperature  $T_{ad}$ , the laminar flame speed  $s_L$  and the thermal flame thickness  $\delta_T$  calculated from the simulations of 1D freely propagating premixed flames as a function of  $\phi$ , at different  $\alpha$ . The calculations were carried out using the OpenSMOKE++ framework [12].

As expected,  $T_{ad}$  increases with increasing  $\phi$  and increasing  $\alpha$ . The higher  $T_{ad}$  of  $\text{H}_2$  may have an impact on the formation of  $\text{NO}_x$ , which are expected to increase with the temperature because of the thermal path. Similarly, also the laminar flame speed  $s_L$  increases with  $\phi$  and  $\alpha$ . More specifically, up to  $\alpha \sim 0.50$ , the increase of  $s_L$  is relatively small if compared to pure  $\text{CH}_4$ . If the  $\text{H}_2$  content increases further, the corresponding increase in  $s_L$  becomes very significant. This is a major issue for practical applications of premixed flames enriched with  $\text{H}_2$ , because the propensity to flashback substantially increases with  $s_L$ . The flame thermal thickness  $\delta_T$  decreases with the reactivity of the mixture, thus with increasing  $\phi$  and  $\alpha$ . Smaller  $\delta_T$  is also expected to promote flashback. Indeed, the quenching distance decreases with  $\delta_T$ ,

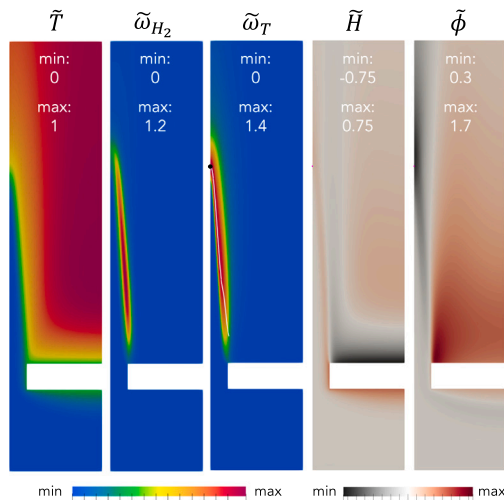


Fig. 3. Scaled temperature  $\tilde{T}$ , hydrogen consumption rate  $\tilde{\omega}_{H_2}$ , heat release rate  $\tilde{\omega}_T$ , enthalpy  $\tilde{H}$ , and local equivalence ratio  $\tilde{\phi}$  at flashback conditions for a pure  $H_2$  flame at  $\phi = 1$  in the reference geometry. The black filled circle identifies the maximum heat release rate and the white line the flame front. The mapped region extends 7.5 mm (2.5 mm) above (below) the burner plate.

so the flame can place itself closer to the wall. Because the fluid velocity decreases as it approaches the wall, flashback is favored. As mentioned in the previous section,  $\delta_T$  is also a quantity of relevance for the 3D simulations, because the cell size adopted in the numerical simulations must be sufficiently small to properly describe it.

### 3.2. Flame structure

An example of flame structure at flashback conditions is available in Fig. 3, which refers to a flame fed with pure  $H_2$  at  $\phi = 1$  (geometry A). The temperature is normalized as  $\tilde{T} = \frac{T - T_u}{T_{ad} - T_u}$ , where  $T_{ad}$  and  $T_u$  are the adiabatic and unburnt gases temperatures, respectively. The enthalpy is normalized as  $\tilde{H} = \frac{H - H_u}{C_{p,u}(T_{ad} - T_u)}$ , where  $H_u$  and  $C_{p,u}$  are the enthalpy and the constant-pressure specific heat of unburnt gases. The local equivalence ratio  $\Phi$  is calculated as:

$$\Phi = \left( \frac{Z_C + Z_H}{Z_O} \right) / \left( \frac{Z_C + Z_H}{Z_O} \right)_{st} \quad (1)$$

and the corresponding scaled value as  $\tilde{\Phi} = \Phi / \Phi_u$ , where  $\Phi_u$  is the equivalence ratio of the unburnt mixture. In the expression above,  $Z_k$  denotes the atomic mass fraction of atom  $k$  and the subscript  $st$  stands for stoichiometric conditions. The  $H_2$  consumption rate and the heat release rate are scaled with the corresponding maximum values in the 1D freely propagating flame at the same equivalence ratio. The location of the maximum heat release rate is indicated by the black filled circle and the flame front is highlighted via a white line defined as the coordinates  $(x_f, y_f)$ , where  $(\mathbf{v} \cdot \nabla \omega_T)_{x_f, y_f} = 0$ . In the expression above,  $\mathbf{v}$  is the flow velocity and  $\omega_T$  the heat release rate.

The scaled temperature field clearly shows that the unreacted gases are significantly pre-heated below the burner plate. More specifically, the increase in scaled enthalpy results from heat conduction in both the preheating zone of the flame (characterized by a significant temperature gradient) and the area in direct contact with the solid material. On the contrary, significant enthalpy losses are present over the top surface of the burner plate. In the core of the flame, changes of enthalpy are less relevant. The map of local equivalence ratio  $\tilde{\Phi}$  reveals very strong preferential diffusion effects, which are especially relevant at the basis of the flame, i.e., close to the top corner of the burner plate, where an increase of  $\tilde{\Phi}$  by  $\sim 50\%$  can be observed. The scaled  $H_2$  consumption  $\tilde{\omega}_{H_2}$  and heat release  $\tilde{\omega}_T$  rates show that the flame burns stronger at

the tip location and along the sides than the unstretched flame. These changes in the local burning rate are associated to preferential diffusion effects induced by stretch [6].

### 3.3. Effect of equivalence ratio

Flashback limits were calculated at different equivalence ratios for the reference geometry. In Fig. 4 we reported the flashback limit cases for pure  $CH_4$  and pure  $H_2$  fuel mixtures, respectively. More specifically, the left side of each maps shows  $\tilde{T}$ , while the right side the map shows  $\tilde{\omega}_T$ . Despite all the flames are stabilized at different values of specific power ( $P_{FB}$ ), the flame height at flashback limits does not change drastically (at the same  $H_2$  content). Only the pure  $H_2$  flame at  $\phi = 0.50$  (not reported in the Figure) exhibits a much shorter length with respect to flames at higher  $\phi$ . As expected, as  $\phi$  decreases, the reaction zone becomes thicker, the flame tip becomes more open and  $\tilde{\omega}_T$  significantly larger, especially close to the flame base region (evidenced by the filled point identifying its maximum). This is a clear indication of stronger preferential diffusion effects at the flame base for leaner conditions. At larger  $\phi$ , the flame front is detached from the wall, by approximately one flame thickness. At lower  $\phi$ , the flame tends to re-attach to the wall, in agreement with the results of Vance et al. [5] on a multi-slit configuration.

### 3.4. Effect of hydrogen content

Fig. 5 shows the maps of  $\tilde{\Phi}$  and  $\tilde{\omega}_T$  at flashback limit conditions for mixtures with  $\alpha$  from 0 to 1 at  $\phi = 0.80$ . As  $H_2$  is added,  $\tilde{\Phi}$  decreases on the centerline, where the flame is curved towards the fresh gases, and increases at the flame basis, where the curvature is the opposite. This is a typical effect for lean mixtures and it is due to the small Lewis number of  $H_2$  ( $Le = 0.316$ ). For pure  $CH_4$  flame, the fuel Lewis number is close to 1 ( $Le = 0.955$ ), which explains why the reduction of  $\tilde{\Phi}$  is much smaller ( $\sim 5\%$ ). Thus, as the hydrogen content is increased, the fuel Lewis number decreases progressively, leading to an increase in the flame height [6].

### 3.5. Analysis of flashback limits

The plots in Fig. 6 shows the specific power at flashback conditions  $P_{FB}$  as a function of the  $H_2$  content for different equivalence ratios (top) and as a function of the equivalence ratio for different  $H_2$  contents (bottom). The propensity to flashback, as expected, increases monotonically with  $\alpha$  and  $\phi$ . However, the increase is relatively small for  $H_2$  fractions below 0.5 and then suddenly increases, especially for large values of  $\phi$ . This appears related to the laminar flame speed reported in Fig. 2, which shows a very similar behavior.

In order to remove the influence of the laminar flame speed, Fig. 7 shows the evolution of the flashback velocity (referred to the hole cross sectional area) normalized over the laminar flame speed. This ratio remains almost constant up to  $\alpha \sim 0.50$ , then it rapidly increases. This confirms the results of Flores-Montoya et al. [6], carried out on a multi-slit configuration, modeled using a planar geometry. This also suggests that the theoretical framework of Lewis and Von Elbe [7] can be considered still valid for flames including a limited amount of  $H_2$ , especially apparent from Fig. 7. As also observed in [5], as the mixture becomes leaner, stronger preferential diffusion effects enhance the flame speed, causing the flashback limit velocities to scale less well with the adiabatic unstretched flame speed. When  $\alpha$  becomes larger than  $\sim 0.5$ , the non-unity Lewis number effects become relevant, causing deviations in the local equivalence ratio which affect the flashback limits. From the analysis of Fig. 7, we also note a non-monotonic behavior in the normalized flashback velocity  $\frac{U_{FB}}{S_L}$  with varying equivalence ratio. A plausible explanation for this phenomenon could be related to the existence of two distinct flashback regimes: at lower  $H_2$  fractions, flashback initiation occurs within the burner hole

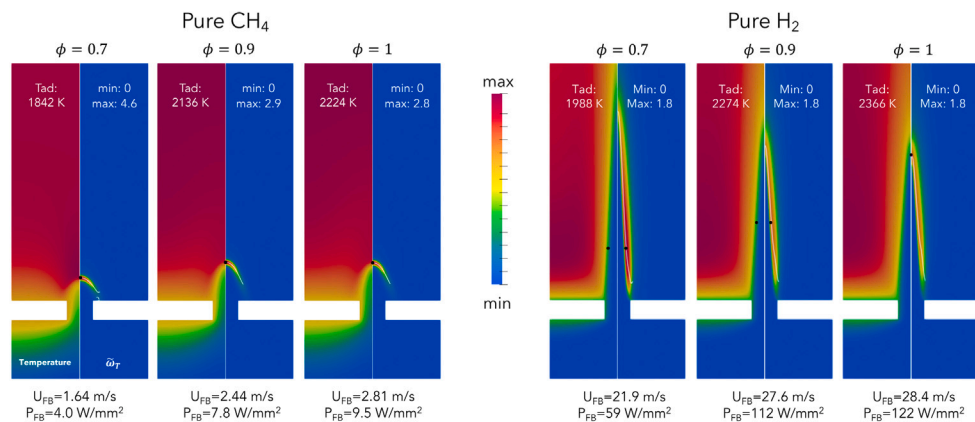


Fig. 4. Maps of  $\tilde{T}$  (left side of each figure) and  $\tilde{\omega}_T$  (right side) for flashback limit cases at different  $\phi$  for pure CH<sub>4</sub> and H<sub>2</sub> flames. At the bottom of each map, the mean velocity through the hole  $U_{FB}$  and the specific power  $P_{FB}$  at flashback conditions are reported. The adiabatic temperature and the maximum value of  $\tilde{\omega}_T$  are also indicated in the maps. The black filled circle identifies the maximum heat release rate and the white line the flame front. The mapped region extends 7.5 mm (2.5 mm) above (below) the burner plate.

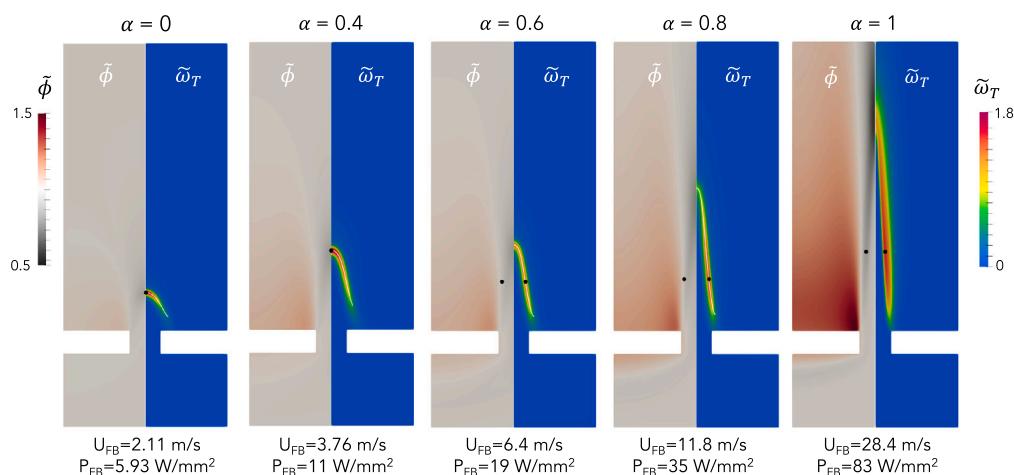


Fig. 5. Maps of  $\tilde{\phi}$  (left side of each figure) and  $\tilde{\omega}_T$  (right side) for flashback limit cases at  $\phi = 0.80$  for different fractions of H<sub>2</sub> in the fuel mixture. At the bottom of each map, the mean velocity through the hole  $U_{FB}$  and the specific power  $P_{FB}$  at flashback limits are reported. The black filled circle identifies the maximum heat release rate and the white line the flame front. The mapped region extends 7.5 mm (2.5 mm) above (below) the burner plate.

due to upstream flame propagation, while at higher H<sub>2</sub> fractions (and perforated plate temperatures sufficiently high), autoignition-driven flashback occurs from below the perforated plate. This hypothesis is also corroborated by the recent experimental results from [16], but it requires additional numerical investigations to be confirmed.

### 3.6. Effect of distance between holes

The effects of the distance between the holes was also investigated. Again, Fig. 8 shows the maps of  $\tilde{\phi}$  and  $\tilde{\omega}_T$  for the pure H<sub>2</sub> flame at  $\phi = 1$  in the three different geometries described in Table 1. We can observe that the flame height significantly decreases with decreasing distance, but the maximum values of both  $\tilde{\phi}$  and  $\tilde{\omega}_T$  are marginally affected by the distance between the holes. Fig. 9 reports the specific power  $P_{FB}$  at flashback conditions as a function of  $\phi$  for pure H<sub>2</sub> flames for the three investigated geometries. We can observe that the flashback limits are a strong function of the distance  $W$  when the equivalence ratio is sufficiently large ( $\phi > 0.50$ ). When  $\phi = 0.50$ , the critical specific power remains basically the same, independently of the distance. This is also apparent by looking at flame heights at  $\phi = 0.50$  (not reported here), which are the same for the three investigated distances. According to [5], this is possibly caused by the higher sensitivity of flame speed to stretch for leaner mixtures, which makes the thermal effect associated to the change in the distance less relevant.

## 4. Conclusions

This study underscores the potential of hydrogen as a key resource for decarbonizing domestic heating systems. The partial substitution of natural gas with hydrogen in domestic combustion-based conversion systems presents an opportunity for improving efficiency, reducing carbon emissions, and achieving cleaner combustion with lower levels of particulate matter. However, the distinctive properties of hydrogen, particularly its higher laminar flame speed, introduce safety concerns related to flashback, emphasizing the need for a thorough investigation.

The focus of this paper was to assess the impact of hydrogen addition to natural gas on the combustion process within domestic condensing boilers. By means of 3D numerical simulations including detailed kinetics and conjugate heat transfer with the burner plate, flashback limits were numerically estimated for multi-hole configurations representative of perforated burners commonly found in domestic boilers.

The obtained flashback limits, spanning equivalence ratios from 0.5 to 1 and hydrogen fractions from 0 (pure methane) to 1 (pure hydrogen), corroborate findings from recent studies on planar, multi-slit configurations. Importantly, the results reveal a limitation in applying the conventional flashback correlation with critical velocity gradient, showing its effectiveness only for a relatively small fraction

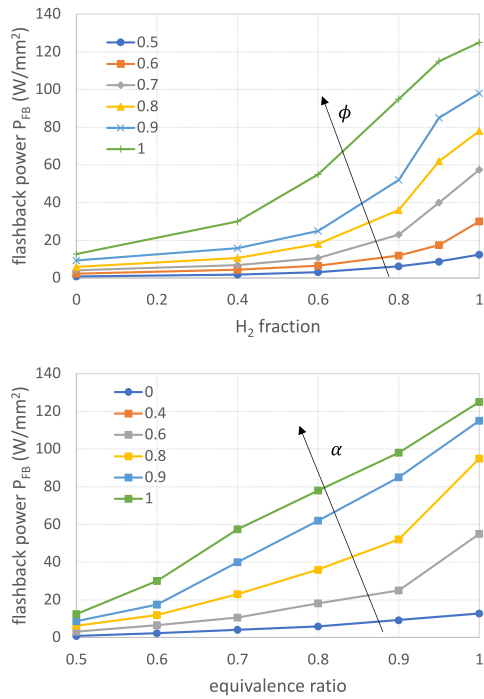


Fig. 6. Specific power at flashback limit as a function of H<sub>2</sub> fraction at different equivalence ratios (top) and as a function of the equivalence ratio at different values of H<sub>2</sub> fraction (bottom).

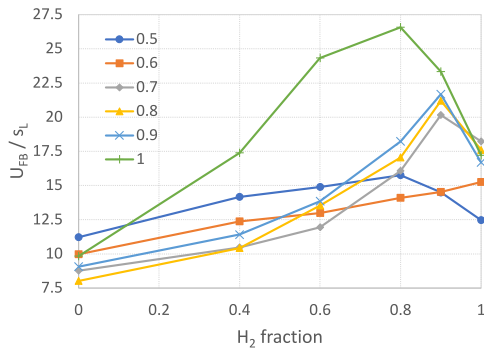


Fig. 7. Ratio between the inlet velocity  $U_{FB}$  and the laminar flame speed  $s_L$  at flashback limit as a function of H<sub>2</sub> fraction at different equivalence ratios.

of H<sub>2</sub> (below 0.50). This limitation is attributed to the oversight of stretch-induced preferential diffusion effects.

In summary, our study provides insights into the flashback limits of H<sub>2</sub>-enriched methane/air premixed laminar flames. The main findings and their implications are outlined below:

- We identified the flashback limits for H<sub>2</sub>-enriched methane/air premixed laminar flames across a range of equivalence ratios (0.5 to 1) and hydrogen fractions (0 to 1). These limits are crucial for the safe operation of domestic burners.
- The addition of H<sub>2</sub> to CH<sub>4</sub> significantly affects the flashback limits due to its higher laminar flame speed and preferential diffusion effects. This finding underscores the need to carefully control H<sub>2</sub> content in fuel mixtures to prevent flashback.
- The multi-hole burner configuration used in this study provides a more realistic representation of practical domestic burners compared to the previously studied multi-slit configurations. This geometric consideration is essential for accurate flashback predictions in real-world applications.

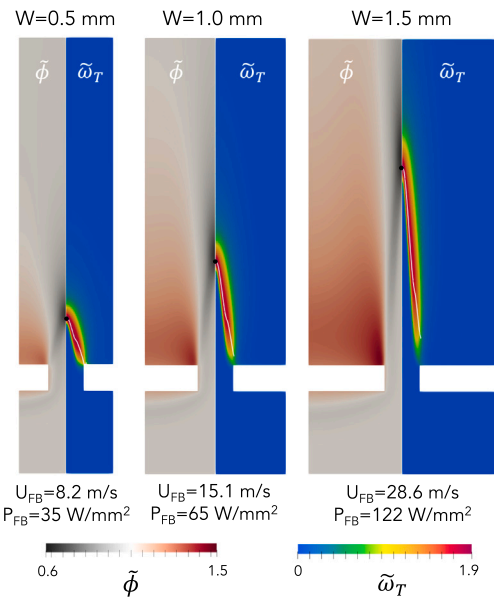


Fig. 8. Scaled equivalence ratio (left side of each map) and heat release rate (right side of each map) for pure H<sub>2</sub> flames in flashback limit cases at  $\phi = 1$  for different distances between the holes. At the bottom of each map, the inlet velocity and the specific power corresponding to flashback limit are reported.

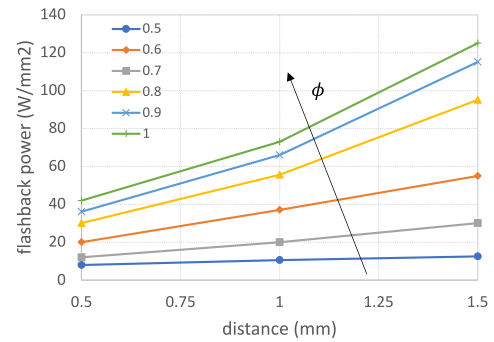


Fig. 9. Specific power  $P_{FB}$  at flashback limit as a function of the distance  $W$  between the holes for the pure H<sub>2</sub> ( $\alpha = 1$ ) flame at different equivalence ratios.

- We observed a non-monotonic relationship between the H<sub>2</sub> fraction and the normalized flashback velocity, which is attributed to preferential diffusion effects.
- The results suggest that conventional flashback correlations may not be adequate for high H<sub>2</sub> fractions, emphasizing the need for revised models that account for preferential diffusion effects.

The insights provided by this study contribute to a better understanding of the combustion process when hydrogen is added to natural gas in domestic condensing boilers. Addressing safety concerns related to flashback and recognizing the limitations of conventional correlations are crucial steps to assess the potential benefits and limitations of hydrogen in achieving cleaner and more sustainable combustion processes in domestic heating systems. Future research should include unsteady simulations to explore more complex phenomena and validate the findings under dynamic conditions relevant to practical applications. This will enhance our understanding of flashback dynamics and improve burner safety and performance.

## Novelty and significance statement

In this research we numerically studied how the addition of hydrogen to methane modifies the flashback limits of lean premixed flames. Similar analyses have been already carried out on 2D multi-slit configurations, but in the present research we considered a 3D multi-hole geometry. This represents a significant novelty and advancement of knowledge. This research is significant because the identification of flashback (which is one of the major concerns about the adoption of H<sub>2</sub> in premixed combustion for domestic applications) was carried out on a 3D multi-hole geometry, which is more representative of perforated burners than the usual 2D multi-slit geometry, adopted in previous works.

## CRediT authorship contribution statement

**A. Cuoci:** Designed research, Performed the numerical simulations, Wrote the paper. **A. Frassoldati:** Analyzed the numerical results. **F. Cozzi:** Analyzed the numerical results.

## Declaration of competing interest

The authors declare that they have no known competing financial interests or personal relationships that could have appeared to influence the work reported in this paper.

## Acknowledgments

The authors acknowledge Prof. Alessandro Stagni from Politecnico di Milano for providing the reduced kinetic mechanism adopted for all the simulations. All authors contributed to revision of the final version of the manuscript.

## References

- [1] Annual Energy Outlook 2023, Energy Information Administration, 2023.
- [2] Natural Gas Annual, Energy Information Administration, 2022.

- [3] Q. Chen, K. Finney, H. Li, X. Zhang, J. Zhou, V. Sharifi, J. Swithenbank, Condensing boiler applications in the process industry, *Appl. Energy* 89 (1) (2012) 30–36.
- [4] R. Lamioni, C. Bronzoni, M. Folli, L. Tognotti, C. Galletti, Feeding H<sub>2</sub>-admixtures to domestic condensing boilers: Numerical simulations of combustion and pollutant formation in multi-hole burners, *Appl. Energy* 309 (2022).
- [5] F.H. Vance, L. De Goey, J.A. van Oijen, Development of a flashback correlation for burner-stabilized hydrogen-air premixed flames, *Combust. Flame* 243 (2022) 112045.
- [6] E. Flores-Montoya, A. Aniello, T. Schuller, L. Selle, Predicting flashback limits in H<sub>2</sub> enriched CH<sub>4</sub>/air and C<sub>3</sub>H<sub>8</sub>/air laminar flames, *Combust. Flame* 258 (2023) 113055.
- [7] B. Lewis, G. Von Elbe, Stability and structure of burner flames, *J. Chem. Phys.* 11 (2) (1943) 75–97.
- [8] A.A. Putnam, R.A. Jensen, Application of dimensionless numbers to flash-back and other combustion phenomena, in: *Symposium on Combustion and Flame, and Explosion Phenomena*, Vol. 3, 1948, pp. 89–98.
- [9] F. Fruzza, R. Lamioni, L. Tognotti, C. Galletti, Flashback of H<sub>2</sub>-enriched premixed flames in perforated burners: Numerical prediction of critical velocity, *Int. J. Hydrog. Energy* 48 (81) (2023) 31790–31801.
- [10] T.B. Kıymaz, E. Böncü, D. Güleriyüz, M. Karaca, B. Yılmaz, C. Allouis, İ. Gökalp, Numerical investigations on flashback dynamics of premixed methane-hydrogen-air laminar flames, *Int. J. Hydrog. Energy* 47 (59) (2022) 25022–25033.
- [11] A. Cuoci, A. Frassoldati, T. Faravelli, E. Ranzi, Numerical modeling of laminar flames with detailed kinetics based on the operator-splitting method, *Energy Fuels* 27 (12) (2013) 7730–7753.
- [12] A. Cuoci, A. Frassoldati, T. Faravelli, E. Ranzi, OpenSMOKE++: An object-oriented framework for the numerical modeling of reactive systems with detailed kinetic mechanisms, *Comput. Phys. Comm.* 192 (2015) 237–264.
- [13] S. Chapman, T.G. Cowling, *The Mathematical Theory of Non-Uniform Gases: an Account of the Kinetic Theory of Viscosity, Thermal Conduction and Diffusion in Gases*, Cambridge University Press, 1990.
- [14] T. Coffee, J. Heimerl, Transport algorithms for premixed, laminar steady-state flames, *Combust. Flame* 43 (1981) 273–289.
- [15] A. Stagni, A. Cuoci, A. Frassoldati, T. Faravelli, E. Ranzi, Lumping and reduction of detailed kinetic schemes: an effective coupling, *Ind. Eng. Chem. Res.* 53 (22) (2014) 9004–9016.
- [16] H. Pers, A. Aniello, F. Morisseau, T. Schuller, Autoignition-induced flashback in hydrogen-enriched laminar premixed burners, *Int. J. Hydrog. Energy* 48 (27) (2023) 10235–10249.